

Chapter 4

The Cohesive Law and Toughness of Engineering and Natural Adhesives

Ahmad Khayer Dastjerdi, Elton Tan, and François Barthelat

Abstract Polymeric adhesives play a critical role in engineering applications, whether it is to bond components together or to serve as matrix for composite materials. Likewise, adhesives play a critical role in natural materials where adhesion is needed (e.g. mussel byssus) or to simply preserve the integrity of natural composite materials by holding fibers together (e.g. extra-collagenous proteins in bone). In this work we use a newly developed technique to measure the cohesive law and toughness of adhesives which is similar to a standard double cantilever beam configuration, but in which the beams are replaced by two rigid blocks. We originally developed this method for extracting the cohesive law of soft and weak biological adhesives, and we here show that it can be modified to include high strength of engineering adhesives. Using this method, the cohesive law of the adhesive is directly computed from the load-deflection curve of the experiment, without making initial assumption on its shape. The cohesive law reveals the strength and extensibility of the adhesives, which is richer in information than the toughness (which is the area under the cohesive law). We also define a non-dimensional parameter which can be used to quantitatively investigate whether the assumption of rigid substrates is valid. For values of the parameter close to unity, the RDCB rigidity assumption is valid and the method directly yields the cohesive law of the adhesive. The engineering and natural adhesives we tested showed a wide range of strength, toughness and extensibility, and revealed new pathways which can be exploited in the design and fabrication of biomimetic materials.

Keywords Adhesives • Fracture toughness • Double-cantilever beam test • Cohesive law • Interfacial adhesion

4.1 Introduction

In recent years, engineering adhesives are increasingly being used in many industries such as automotive and aerospace for bonding various structures [1, 2]. In comparison with classical joining methods such as fastening or spot welding, adhesive joints provide distinct advantages which enable them to be extensively used in a variety of technological and industrial applications. Bonded components transfer stresses more uniformly even if they are made of dissimilar materials, and a glued joint is lighter and less expensive than other traditional joining methods [1]. The main failure mode of adhesive joints is shearing, and the most common testing method to characterize their performance is shear lap test, yielding the strength of the interface [3]. Despite the fact that the strength of an adhesive interface is a key factor controlling its mechanical performance, it is now well-understood that the strength of a material can highly be affected by presence of defects and flaws which may form due to inaccurate joint assembly or inappropriate curing; these defects under certain loading condition may propagate into large crack and eventually lead to its failure. It is therefore essential to characterize and evaluate the toughness of the bond line, which directly affects strength, reliability and energy absorption of the material. Several experimental techniques have so far successfully designed and employed to measure the fracture toughness of adhesive joints under mode I fracture loading (opening mode) which include double cantilever beam (DCB) test [4, 5], blister test [6], and indentation test [7, 8]. Amongst them, the DCB test, developed by Ripling and Mostovoy [4] has gained considerable popularity owing to its relative simplicity of analysis and

A. Khayer Dastjerdi • E. Tan • F. Barthelat (✉)
Department of Mechanical Engineering, McGill University, Montreal, QC, Canada
e-mail: ahmad.khayerdastjerditoroghi@mail.mcgill.ca; elton.tan@mail.mcgill.ca; francois.barthelat@mcgill.ca

easiness of sample preparation. This test method has also been adopted as an ASTM standard [9]. A DCB specimen consists of two rectangular beams, of uniform thickness, bonded together by a thin layer of adhesive in such a way that one end of the beams remains free of the adhesive. The specimen is then loaded by pulling the free ends of the two beams in a direction normal to the fracture surface, so that a crack extends along the interface of the two beams. The elastic energy which is stored in the deformed portion of the beams and released upon crack extension is calculated to measure the toughness (energy required to extend a crack) of the adhesive [4, 10].

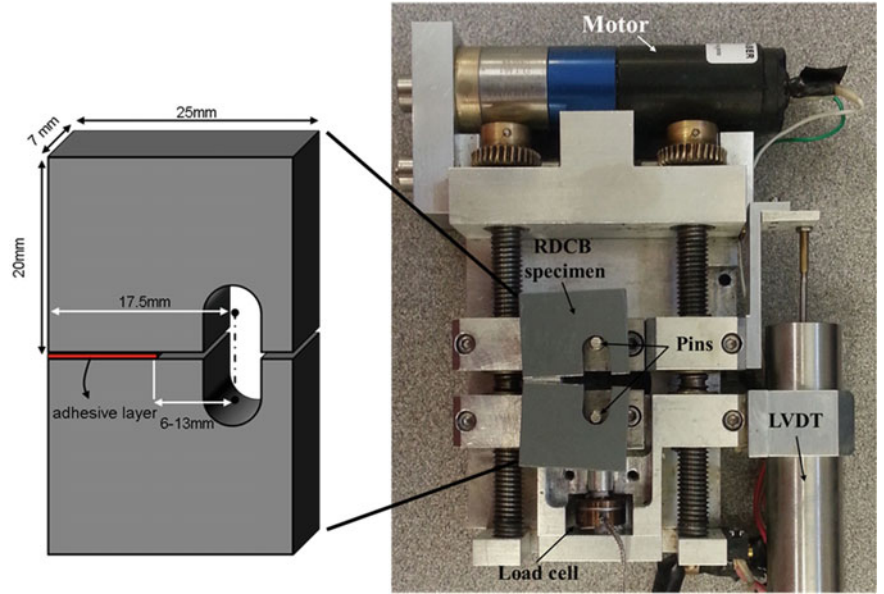
The basic DCB method can be combined by other experimental techniques for example in-situ imaging to obtain the cohesive law (traction-separation function) of adhesives [11–16]. The cohesive law of the adhesive can then serve as the basis for cohesive zone modeling (CZM), which is a powerful technique to simulate crack initiation and growth often used to model fracture and fragmentation processes in metallic, polymeric, and ceramic materials and their composites [17–19]. In order to propagate the crack by an increment of distance, the cohesive forces will produce work over the opening distance, so that the toughness (in terms of energy per unit surface) is simply obtained by measuring the area under the cohesive law. The full cohesive law provides more information (including the maximum traction exerted by adhesive on the crack walls, stiffness of the adhesive layer, and maximum separation prior to the final de-cohesion) than a simple measurement of toughness.

The experimental determination of full cohesive laws is more involving than measuring toughness and requires more experimental and/or numerical elaborations. The developed methods for cohesive law determination are generally classified into two main categories: direct and inverse techniques. In direct methods, cohesive law is essentially obtained from the results of fracture experiments [11–13, 20–22] and using the concept of J-integral approach. While these techniques are valuable, they, however, are expensive in terms of experimental procedure and often need additional experimental setup. The inverse methods represent another type of approach which consists in modeling the experiment using finite elements, and identifying the parameters of the cohesive law which produce the best match between the model and the experiments [11, 23–25]. In general, direct and indirect methods assume a shape for the cohesive law, typically a bi-linear function (triangular cohesive law), which is characterized by three independent parameters (for example strength, maximum opening and toughness). In spite of the usefulness of these techniques, a method to directly measure cohesive laws without experimental and numerical complications is needed. In this article, we present a novel and simple experimental technique to measure the cohesive law of engineering adhesives. First developed to measure the interfacial fracture toughness of soft, weak biological adhesives [26], this technique is not modified to determine the cohesive law of tough, strong engineering adhesives. The new rigid-double-cantilever-beam (RDCB) technique is similar in concept to the standard DCB test, with an important difference: the substrates are assumed to be rigid. In the RDCB configuration the strain energy eventually released upon crack propagation is therefore stored in the adhesive itself. The assumption of rigid substrates also means that the opening of the adhesive can be easily computed along the entire bond line, without the need for contact or non-contact optical extensometers. The analysis for this test is also extremely simple, and directly leads to the full cohesive law of the adhesive, without any initial assumption on its shape.

4.2 RDCB Test Setup and Sample Preparation

Test setup of the rigid-double-cantilever-beam (RDCB) experiment is relatively similar to the traditional DCB test but the substrates are considered to be sufficiently stiff with respect to the adhesive as they can be assumed rigid. Here we used two rigid steel blocks (with the geometries shown in Fig. 4.1) as substrate for adhesives to be studied. The adherent surface was mirror polished down to 0.05 μm particle size in order to ensure a smooth surface, minimizing the effect of roughness on the results. We did not study rougher surfaces in this work, while they can easily be tested using RDCB method. The adhesive was used to join the two blocks, by partially covering their interfaces. The prepared specimen was then placed on a miniature loading stage (Fig. 4.1). An opening displacement at a rate of 50 $\mu\text{m/s}$ was applied on the RDCB specimen using two steel pins (Fig. 4.1). The applied load and displacement were measured during the experiment using a 100 lbs load cell and one LVDT, respectively. The compliance of the machine was independently measured by mounting a calibration sample consisting of a single steel block with the same overall dimensions and the same slot as shown in Fig. 4.1, but with no interface. All the experimental curves reported here were then corrected for machine compliance.

Fig. 4.1 Schematic illustration of the RDCB sample geometry (*left*); actual picture of the setup showing an opened sample mounted on the miniature loading stage (*right*)



4.3 RDCB Test Analysis

The key part in RDCB analysis is the assumption of a rigid substrate compared to the deformable adhesive. In order to meet this assumption, the deformation of the substrate during the course of the loading should be negligible compared to that of the adhesive layer. We further discuss the validity of this assumption in Sect. 3. Since the substrates are considered to be rigid, they only rotate about the hinge point O located at the end of the beams (Fig. 4.2). This assumption enables us to directly calculate the opening of the interface $u(x)$ anywhere along the bond line:

$$u(x) = \frac{x}{L} \Delta \quad (4.1)$$

Where x is the position from the hinge point, L is the distance from the line of action of the pulling force to the hinge point O , and Δ is the pins separation displacement. Writing the balance of moment (about the hinge point) exerted by the closure force of the adhesive with the moment generated by the applied external load F yields:

$$B \int_0^b xt(x)dx = LF \quad (4.2)$$

Where B is the thickness of the substrates, b is the length of the bond line, and $t(x)$ denotes the traction function which is unknown and is to be determined. Since the opening along the entire length of the substrates is known, we can now use Eq. 4.1 for a change of variable in Eq. 4.2, yielding:

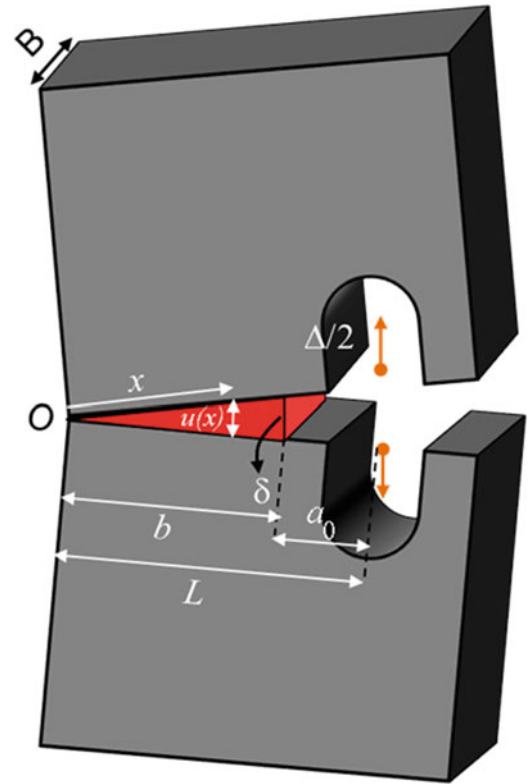
$$\left(\frac{L}{\Delta}\right)^2 \int_0^\delta ut(u)du = \frac{L}{B}F \quad (4.3)$$

Where δ is the separation at the crack tip. Differentiating from Eq. 4.3 with respect to δ and using $\delta = \frac{b}{L} \Delta$ lead to the traction function of the adhesive layer, as follows:

$$t(\delta) = \left(\frac{L}{B(L - a_0)^2}\right) \left(2F + \Delta \frac{dF}{d\Delta}\right) \quad (4.4)$$

This equation simply gives the cohesive law of the interface from the traction function of the load–displacement curve and its derivative, and from the geometry of the specimen. Unlike many other methods developed to determine the cohesive

Fig. 4.2 Schematic illustration of a RDCB specimen with relevant variables used here for analysis



law of the adhesive interfaces, Eq. 4.4 does not require any initial assumption on the shape of the cohesive law which is a significant advantage. When the cohesive law is determined, the fracture toughness of the interface can simply be calculated by the area under the cohesive law which is also called cohesive energy:

$$J_{IC} = \int_0^{\infty} t(u) du \quad (4.5)$$

The toughness obtained from Eq. 4.5 is equal to the work-of-fracture, defined as the area under the $F-\Delta$ divided by the initial surface area of the adhesive (i.e. work-of-fracture measures the energy required to separate a unit surface of adhesive).

We also validated the result of the presented RDCB model by testing a 1 mm-thick double-sided polyethylene foam adhesive tape sandwiched between two steel substrates. Using Eq. 4.4, the obtained $F-\Delta$ curves yielded the cohesive law of the tape. Equation 4.5 was then used to compute the toughness of the tape which was $J_{IC} = 116 \pm 21 \text{ J/m}^2$ (five samples were tested). We also measured the toughness of this adhesive (taped on the same polished steel surface) using a standard peel test configuration (ASTM D6862-04) which gave a toughness of $J_{IC} = 127 \pm 15 \text{ J/m}^2$ (five specimens were tested). The values given by the RDCB and peel tests are comparable within experimental errors, which validated the RDCB test procedure and data analysis.

4.4 Rigidity Assumption Validation

We noted earlier that the RDCB model relies on the assumption of a rigid cantilever compared to the adhesive. In order to verify the validity of this assumption, the deformation of the substrate must be negligible compared to the deformation of the adhesive interface. Since the highest deformation occurs when the interface passes the yield point of the cohesive law, it is sufficient to compare the deflection of the substrates and adhesives at the end of the elastic regime.

In order to identify the critical parameters governing the deflection of the substrate and the adhesive, we consider the free body diagram of the upper substrate (Fig. 4.3). The opening force was modeled as point load, and the adhesive was modeled

Substituting the shear loads and bending moments from Eq. 4.9 into Eq. 4.8, and taking derivative from Eq. 4.8 with respect to P yields the deformation of the substrate at the loading line:

$$\delta_1 = P \left(\frac{\alpha_s}{GA} + \frac{\alpha_b}{EI} \right) \quad (4.10)$$

With $\alpha_s = \frac{9}{5}L \left(\frac{L}{b} - 1 \right)$ and $\alpha_b = \left(\frac{L^3}{3} + \frac{Lb^2}{10} - \frac{2L^2b}{5} \right)$. By assuming a homogeneous isotropic linear elastic property for the substrate material (with rectangular cross section), Eq. 4.10 can further be simplified as:

$$\delta_1 = \frac{P((1+\nu)\alpha'_s + \alpha'_b)}{E} \quad (4.11)$$

With $\alpha'_s = \frac{2\alpha_s}{Bh}$ and $\alpha'_b = \frac{12\alpha_b}{Bh^3}$. Where ν and h denote the poisson's ratio and thickness of the substrate, respectively. In addition to this opening, resulting from bending moments and from shear forces, the adhesive layer separation also produces opening along the loading line which must be considered in the calculations. This is taken into account by rotating the substrate around the hinge point O so that the crack tip opens up to $2\delta_{tip}$ which gives:

$$\delta_2 = \left(\frac{L}{b} \right) \delta_{tip} \quad (4.12)$$

Adding the opening from Eqs. 4.11 and 4.12 gives the total substrate tip opening:

$$\Delta' = P \left(\frac{(1+\nu)\alpha'_s + \alpha'_b}{E} + \frac{3L^2}{Bb^3S_{int}} \right) \quad (4.13)$$

We now define a non-dimensional ratio $\alpha = \frac{\delta_{tip}L}{\Delta'b}$ which can be used to assess the rigidity of the substrate. This ratio must be equal, or close to unity for the substrate to be considered rigid. In this case the surface of the substrate remains uniformly straight and Eq. 4.1 can be used. Substituting half the crack tip opening from Eq. 4.7 and the substrate tip opening from Eq. 4.13 into this ratio results:

$$\alpha = \frac{\delta_{tip}L}{\Delta'b} = \left(1 + \frac{Bb^3S_{int}((1+\nu)\alpha'_s + \alpha'_b)}{3L^2E} \right)^{-1} \quad (4.14)$$

This equation can now be used to verify the rigidity assumption of the substrates. It incorporates the geometry of the specimens, as well as the elastic properties of the substrate and the cohesive strength of the adhesive layer. Using this equation, we plotted the ratio α as a function of dimensionless material parameter σ_m/E (ratio of the cohesive strength of the interface to the modulus of the substrate) for the fixed dimensions specified in Fig. 4.1 (Fig. 4.4). The model confirms that the ratio is equal to one for low cohesive strength of the adhesive and/or high substrate modulus. When the ratio σ_m/E gets larger, α deviates from unity, indicating substrate deformation. α becomes smaller than 0.95 for $\sigma_m/E > 8.3 \times 10^{-4}$. As the ratio α becomes larger the traditional DCB method becomes more appropriate.

Finally Eq. 4.14 was verified using finite element method. We constructed the RDCB configuration in ABAQUS (v. 6.9, ABAQUS Inc., Providence, RI), with the geometry shown in Fig. 4.1. Using symmetry about the plane defined by the bond line, only the upper half of the system was modeled: one substrate, and half of the thickness of the bond line. The substrate was modeled as linear elastic with plane strain condition. The interface was modeled with user defined cohesive elements, with the upper nodes joined with the node from the substrate, and the lower nodes only constrained to remain on the plane of symmetry. A trapezoidal cohesive law was chosen to simulate crack propagation within the adhesive layer. The upper pin of the fixture was modeled as a rigid surface in contact with the inner surface of the fixture. The pin was displaced at a fixed rate to simulate the opening of the interface. Figure 4.4 shows a good agreement between the finite element results and the analytical result of Eq. 4.14, validating the accuracy of the presented analytical method.

Fig. 4.4 α as a function of dimensionless parameter $\frac{\sigma_m}{E}$ showing intimate agreement between results obtained from finite element and from analytical model (Eq. 4.14)

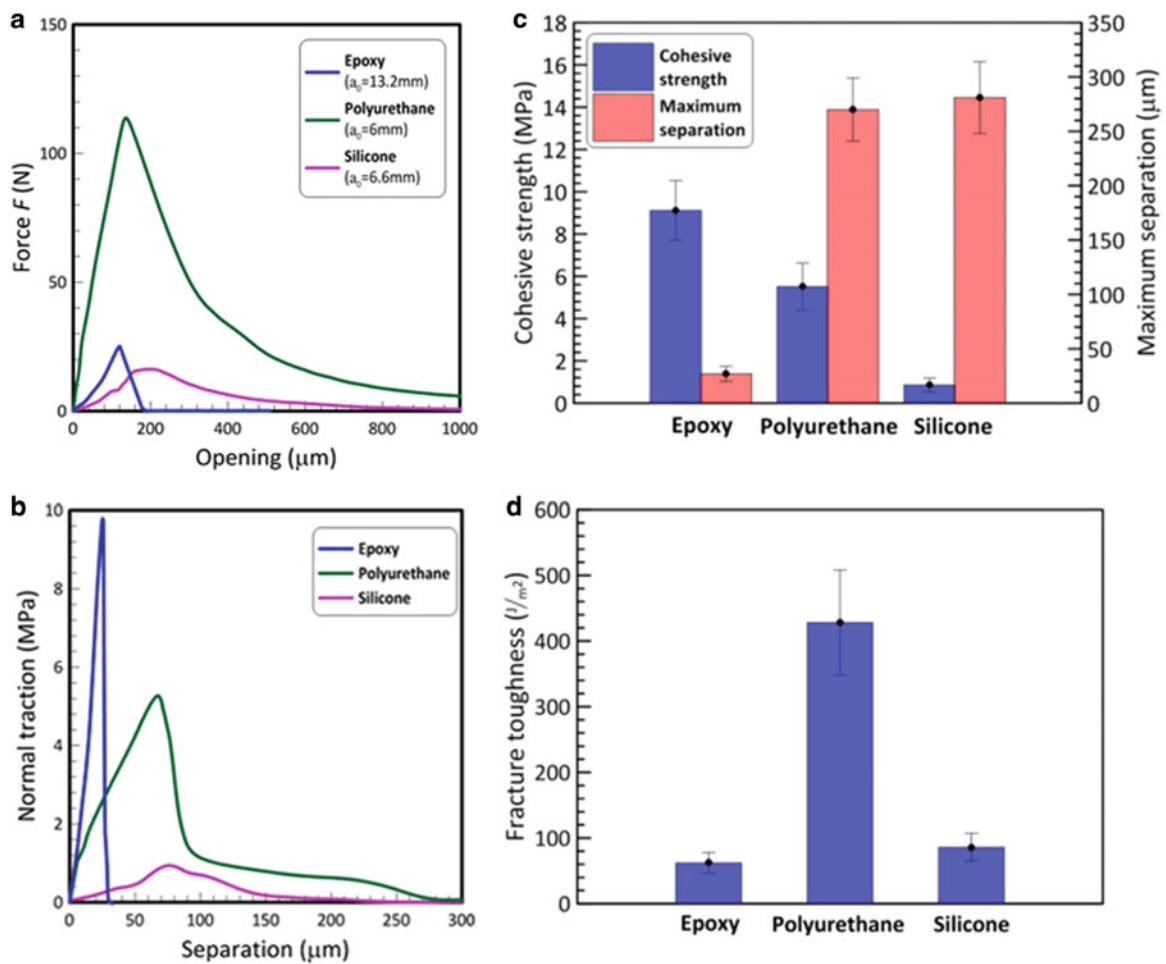
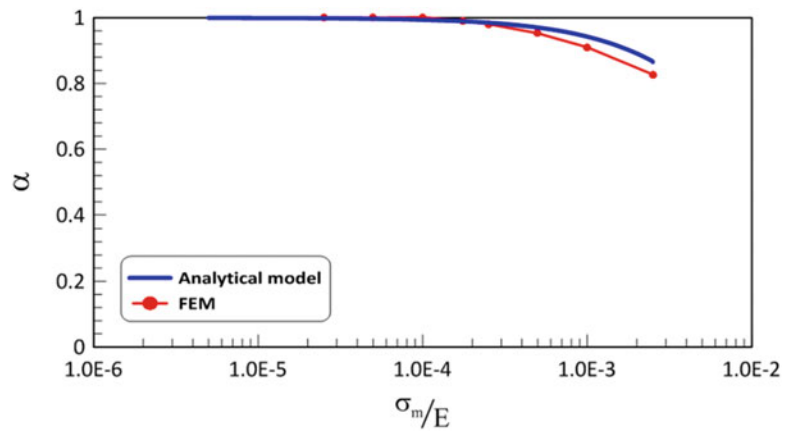


Fig. 4.5 Typical force-opening curves of the three tested types of adhesive; (b) typical cohesive laws obtained from RDCB model; (c) cohesive parameters for the three adhesive tested in this work: (a) cohesive strength and maximum separation, and (d) toughness

4.5 RDCB Test on Typical Engineering Adhesives

Using RDCB method we tested three engineering adhesives with a wide range of mechanical behavior from soft elastomer to stiff thermoset polymer: silicone (Silicone, General Electric, Huntersville, NC, USA), polyurethane (PL Premium, Lepage, Brampton, ON, Canada), and epoxy (EpoThin epoxy, Buehler, Lake Bluff, IL, USA). Typical load-opening curves resulting from RDCB tests on each of these three adhesives are shown in Fig. 4.5a. Polyurethane and epoxy showed a linear increase

at the initial part of the loading which is followed by an almost abrupt drop corresponding to the onset of crack propagation. For the case of silicone, the failure process was more progressive exhibiting a bell shape force-opening curve. Using optical microscope, posttest fracture surface of the specimens was further explored. The fracture surfaces of epoxy and silicone clearly indicated adhesive failure (the crack propagated at the adhesive-substrate interface) along one interface. Polyurethane displayed a mixed failure mode including cohesive failure, adhesive failure (the crack propagated through the adhesive) and crack deflections. From a fracture mechanics perspective, the latter failure mode is more desirable because it involves more energy dissipation, which translates into increased fracture toughness for the interface. The obtained force-opening curves were then processed through RDCB analysis explained in Sect. 2; the typical cohesive laws for the three studied adhesives are shown in Fig. 4.5b. This data was used to measure the cohesive strength of the adhesive (maximum traction) and the maximum separation (opening at which the cohesive law vanishes). Figure 4.5c presents the average values of these cohesive law parameters. Epoxy was the strongest but also the most brittle of the three adhesives, with a cohesive strength of 8–10 MPa and maximum opening of about 25 μm . In contrast, silicone showed a low cohesive strength about 10 times lower (1 MPa) but a maximum separation about 10 times larger than epoxy.

Figure 4.5d presents the toughness of the adhesives which was obtained from Eq. 4.5. Amongst all the tested adhesives, polyurethane is the toughest with average fracture toughness being approximately 430 J/m^2 . This was predictable from parameters (cohesive strength and maximum separation) shown in Fig. 4.5c, because it exhibits both high strength and large extensibility. Epoxy and silicone (despite being either strong or deformable) display low fracture toughness mainly due to the shortage of extensibility (in epoxy) and strength (in silicone). In order to investigate the validity of the results we obtained for these adhesives using RDCB model, we determined the ratio α (Eq. 4.14) for each case. For all the cases, parameter α is approximately unit (maximum deviation from unit happens in the case of epoxy adhesive which is 0.3%) which confirms that all the results presented in this study are valid and can be used for further studies on the fracture behavior of the adhesives.

4.6 Conclusions

In this study, a simple yet robust experimental method called RDCB test was presented to determine the cohesive law and fracture toughness of engineering adhesive in the opening fracture case (Mode I). First developed for soft, deformable biological adhesives, RDCB method can be modified to include high strength of tough engineering adhesives using thick rigid substrates. The method is very useful and unlike many other developed techniques needing an initial assumption for the shape of the cohesive law and requiring complex experimental setup, imaging or numerical modeling, RDCB test provides the full cohesive law of the adhesive without any initial assumption on its shape. The method only needs the initial geometry of the specimen as well as the load–displacement data from experiment. In order to validate the results of the model, we defined a non-dimensional parameter called α which can be used to quantitatively investigate whether the assumption of rigid substrates is valid. For values of α close to unity, the RDCB rigidity assumption is valid and the method directly yields the cohesive law of the adhesive. Finally we successfully implemented the RDCB method on three typical engineering adhesives: epoxy, polyurethane and silicone. The results showed very different cohesive laws for these adhesives. Epoxy showed high cohesive strength but small extensibility, while silicone showed high extensibility but low strength. Polyurethane, with both high strength and extensibility, was found to be the toughest of the adhesives tested here. The RDCB method is a simple and accurate method to obtain the cohesive law of adhesives, and can serve as an experimental platform to investigate their mode of failure or to optimize their performance.

Acknowledgements This work was supported by a Discovery Grant from the Natural Sciences and Engineering Research Council of Canada. AKD was partially supported by a McGill Engineering Doctoral Award.

References

1. Adams R, Comyn J, Wake W (1997) Structural adhesive joints in engineering. Chapman and Hall, London
2. Dunn DJ (2004) Engineering and structural adhesives, vol 169. Smithers Rapra Technology, Shrewsbury
3. ASTM (1986) ASTM D 3983: Standard test method for measuring strength and shear modulus of nonrigid adhesives by the thick-adherent tensile-lap specimen. West Conshohocken, PA, pp 412–428
4. Ripling EJ, Mostovoy S, Corten HT (1971) Fracture mechanics: a tool for evaluating structural adhesives. *J Adhes* 3(2):107–123
5. Dastjerdi AK et al (2012) Cohesive behavior of soft biological adhesives: experiments and modeling. *Acta Biomater* 8(9):3349–3359

6. Dannenberg H (1961) Measurement of adhesion by a blister method. *J Appl Polym Sci* 5(14):125–134
7. Chicot D, Démarécaux P, Lesage J (1996) Apparent interface toughness of substrate and coating couples from indentation tests. *Thin Solid Films* 283(1–2):151–157
8. Lawn BR (1993) *Fracture of brittle solids*. Cambridge University Press, Cambridge, United Kingdom
9. ASTM (2012) ASTM D3433–99: Standard test method for fracture strength in cleavage of adhesives in bonded metal joints. West Conshohocken, PA
10. Anderson TL (1995) *Fracture mechanics: fundamentals and applications*. CRC Press, Boca Raton, FL
11. Andersson T (2006) On the effective constitutive properties of a thin adhesive layer loaded in peel. *Int J Fract* 141(1–2):227
12. de Moura M (2012) A straightforward method to obtain the cohesive laws of bonded joints under mode I loading. *Int J Adhes Adhes* 39:54
13. Biel A (2010) Damage and plasticity in adhesive layer: an experimental study. *Int J Fract* 165(1):93
14. Sørensen BF (2003) Determination of cohesive laws by the J integral approach. *Eng Fract Mech* 70(14):1841
15. Carlberger T, Stigh U (2010) Influence of layer thickness on cohesive properties of an epoxy-based adhesive—an experimental study. *J Adhes* 86(8):816–835
16. Zhu Y, Liechti KM, Ravi-Chandar K (2009) Direct extraction of rate-dependent traction-separation laws for polyurea/steel interfaces. *Int J Solids Struct* 46(1):31–51
17. Shet C, Chandra N (2002) Analysis of energy balance when using cohesive zone models to simulate fracture processes. *J Eng Mater Technol Trans Asme* 124(4):440–450
18. Bouvard JL et al (2009) A cohesive zone model for fatigue and creep–fatigue crack growth in single crystal superalloys. *Int J Fatigue* 31(5):868–879
19. Aymerich F, Dore F, Priolo P (2009) Simulation of multiple delaminations in impacted cross-ply laminates using a finite element model based on cohesive interface elements. *Compos Sci Technol* 69(11–12):1699–1709
20. Barthelat F et al (2007) On the mechanics of mother-of-pearl: a key feature in the material hierarchical structure. *J Mech Phys Solids* 55(2):306–337
21. Sørensen BF (2002) Cohesive law and notch sensitivity of adhesive joints. *Acta Mater* 50(5):1053
22. Andersson T (2004) The stress–elongation relation for an adhesive layer loaded in peel using equilibrium of energetic forces. *Int J Solids Struct* 41(2):413
23. de Moura MFSF, Morais JLL, Dourado N (2008) A new data reduction scheme for mode I wood fracture characterization using the double cantilever beam test. *Eng Fract Mech* 75(13):3852
24. Sun C et al (2008) Ductile–brittle transitions in the fracture of plastically-deforming, adhesively-bonded structures. Part I: experimental studies. *Int J Solids Struct* 45(10):3059–3073
25. Sun C et al (2008) Ductile–brittle transitions in the fracture of plastically deforming, adhesively bonded structures. Part II: numerical studies. *Int J Solids Struct* 45(17):4725–4738
26. Khayer Dastjerdi A et al (2012) The cohesive behavior of soft biological “glues”: experiments and modeling. *Acta Biomater* 8:3349
27. Timoshenko S (1940) *Strength of materials Part 1: Elementary theory and problems*. (2nd edn) D. Van Nostrand Company Inc., New York